New Insights into the Role of Transient Chiral Mediators and Pyridone Ligands in Asymmetric Pd-Catalyzed C-H Functionalization

David E. Hill, †,‡ Jin-Quan Yu,† Donna G. Blackmond*†

ABSTRACT: Mechanistic investigations uncover a novel role for 2-pyridone ligands and interrogate the origin of enantioselectivity in the (+)-norbornene mediated Pd-catalyzed *meta*-C(aryl)–H functionalization of diarylmethylamines. Observations from kinetics analysis in concert with *in-situ* ¹⁹F NMR monitoring allow us to propose that the pyridone ligand plays a role in enhancing the rate-and enantio-determining insertion of an arylpalladium species into a chiral norbornene derivative. The unprecedented features of 2-pyridone ligands in asymmetric 1,2 migratory insertion, and norbornene as a transient chiral mediator in relay chemistry, provide new insights into this ligand scaffold for future developments in stereoselective transition-metal catalyzed C–H functionalization.

INTRODUCTION

Pd-catalyzed C-H functionalization methodologies promoted by 2-pyrdione ligands have become prominent in recent years. 1-⁹ This class of Pd-catalysis was initially discovered to facilitate norbornene mediated meta-C(aryl)-H functionalization¹ and then later developed to perform the Fujiwara–Moritani reaction using the arene substrate as a limiting reagent⁵, a long-standing challenge in non-direct C-H activation. Although the norbornene-mediated relay of ortho-cyclopalladation to the metaposition of an aryl ring system is a well-established process in the Catellani reaction, 10-11 the use of norbornene as a transient chiral mediator to control stereoselectivity in C-H activation is a new approach developed by the Yu group.⁷ The origin of the enantioselectivity for this novel stereoselective meta-C(aryl)–H functionalization remains speculative. The 2-pyridone ligand scaffold was originally conceived as a potential surrogate in lieu of acetate and was hypothesized to act as an improved internal base for promoting C-H bond cleavage (Scheme 1).1 Experimental and computational studies of non-directed Pd-3,5-ditrifluoromethyl-2-pyridone-catalyzed C-H functionalization by the Yu group have suggested that the 2-pyridone ligand could accelerate C-H activation by lowering the energy barrier for concerted-metalation deprotonation as well as prevent catalyst degradation by forming a stable trimeric Pd-pyridone complex.5

Scheme 1. Role of Pyridone as an Acetate Surrogate in C–H Functionalization.

These striking mechanistic features of 2-pyridone ligands and the chiral norbornene transient mediator prompted us to study the reaction in Scheme 2, norbornene-mediated Pd-2-pyridone-catalyzed *meta*-C(aryl)–H functionalization. This investigation

reports mechanistic studies supporting previous work as well as presenting novel mechanistic understanding of the catalyst resting state and the enantio-controlling step for Pd-catalyzed (+)-norbornene mediated *meta*-C(aryl)–H functionalization. These findings could enable further development of norbornene mediated *meta*-C(aryl)–H functionalization.

Scheme 2: Asymmetric Pd-norbornene (4)-pyridone (5)-catalyzed C–H arylation of diarylmethylamines.⁷

RESULTS AND DISCUSSION

Our mechanistic investigation of the Pd-catalyzed C(aryl)—H arylation of biarylmethylamines (Scheme 2) began with probing the kinetic behavior of the reaction by simultaneously measuring the consumption of substrate 1 and the formation of reaction product 3, revealing a temporal loss of reaction mass balance and an increase in % *e.e.* of product 3 from 76% to 90% as the reaction proceeds to high conversion of 1 (Figure 1). Further analysis of the reaction mixture led to the detection of a Pdnorbornene (4)-pyridone (5)-catalyzed C(aryl)—H double arylation side reaction to yield 7 (Scheme 3). This undesirable process forming 7 accounts for the missing mass and was hypothesized to occur through the kinetic resolution of product 3 in a second aryl addition. Studies monitoring the reaction of racemic product (±)-3 yielded a temporal increase in the % *e.e.* of 3,

[†] Department of Chemistry, The Scripps Research Institute, La Jolla, California 92037, United States

from which we calculate that the arylation of 3 to form 7 occurred through a kinetic resolution process with a selectivity factor of s=7. Therefore, to establish kinetic dependences of substrates in this reaction, we chose to interrogate the intrinsic kinetics of this reaction by monitoring the consumption of 1.

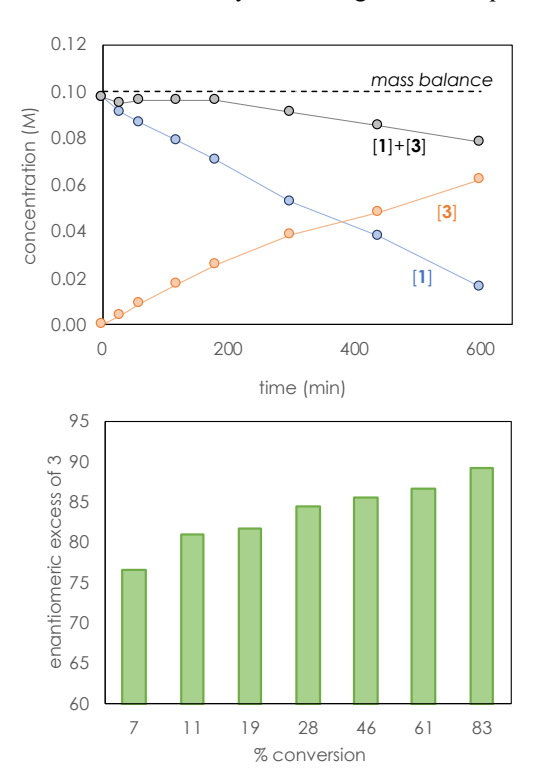


Figure 1: Reaction progress data for reaction of Scheme 2 (top). Temporal monitoring of 3 % *e.e.* (bottom).

Scheme 3. Kinetic Resolution Via Second Arylation of Product 3.

Experiments aimed at determining the catalyst robustness and concentration dependencies of each reaction component were conducted according to the same excess and different excess protocols of Reaction Progress Kinetic Analysis (RPKA)¹²⁻¹³ with the term "excess" defined by Equation 1. Figure 2 shows the kinetics profiles for experiments carried out using the same excess protocol. The time-adjusted curves, as indicated by the arrow in Figure 2, enable the comparison of the kinetic profiles for the two experiments as they react under identical substrate conditions onward from the point of intersection of the arrows. The overlay of these two reaction profiles indicates that the reaction rate under standard conditions is not influenced by either the additional catalyst turnovers completed or the presence of products 3 or 7 in the reaction vial, compared to the fresh

conditions of the same excess experiment. This observation of overlay for experiments of same excess confirms that the absence of both irreversible catalyst deactivation and product catalyst inhibition during catalysis.

$$[excess] = [2]_0 - [1]_0$$
 (1)

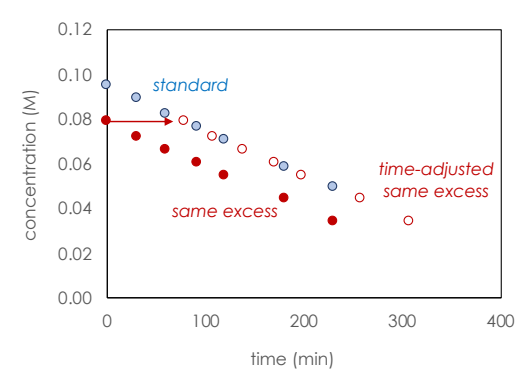


Figure 2: Kinetic profile for C–H arylation reaction shown in Scheme 1 plotted as [1] against time carried out using the same excess procedure with [excess] = 0.2 M. Both reactions with $[Pd(OAc)_2] = 0.01$ M, [4] = 0.02 M, [5] = 0.015 M, and 3.0 equiv. of AgOAc in chloroform at 80 °C. (blue circles) [1]₀ = 0.1 M; [2]₀ = 0.3 M. (red circles) [1]₀ = 0.08 M; [2]₀ = 0.28 M. (red non-filled circles) time-adjusted data from red circles.

After confirming the robustness of the Pd catalyst, we next interrogated the concentration driving forces of the reaction through different excess experiments. The data for the different excess experiments in Figure 3 demonstrates zeroth order rate dependence for both substrates [1] and the [2]. First order rate dependence on $[Pd(OAc)_2]$ and [4] co-catalyst were revealed via Variable Time Normalization Analysis¹⁴ (Figures 4 and 5). Overlay between the profiles indicates the order in both [Pd] and [4] shows n = 1, or first order dependence in each case. We also established the lack of a nonlinear effect on product ee as a function of [4].

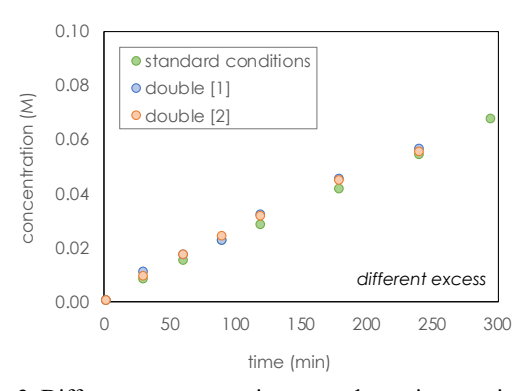


Figure 3: Different excess experiments to determine reaction order in [1] and [2] plotted as the assumed [3] against time. All reactions with $[Pd(OAc)_2] = 0.01 \text{ M}$, [4] = 0.02 M, [5] = 0.015 M, and 3.0 equiv. of AgOAc in chloroform at 80 °C. (blue circles) [1]₀ = 0.1 M; [2]₀ = 0.3 M. (red circles) [1]₀ = 0.1 M; [2]₀ = 0.6 M. (green circles) [1]₀ = 0.2 M; [2]₀ = 0.3 M.

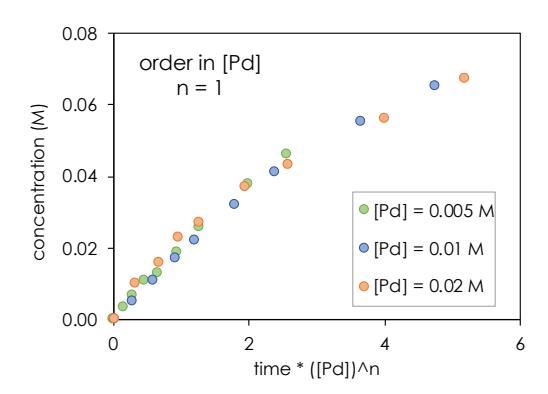


Figure 4: Variable Time Normalization Analysis (VTNA)¹⁴ for reactions containing varied $[Pd(OAc)_2]$ plotted as the assumed [3] against normalized-time. All reactions contain [4] = 0.02 M, [5] = 0.02 M, [1]₀ = 0.1 M, [2]₀ = 0.3 M, and 3.0 equiv. of AgOAc in chloroform at 80 °C. (blue circles) [Pd(OAc)] = 0.01 M. (red circles) [Pd(OAc)] = 0.02 M. (green circles) [Pd(OAc)] = 0.005 M. Overlay for n=1 signifies first order kinetics in [Pd].

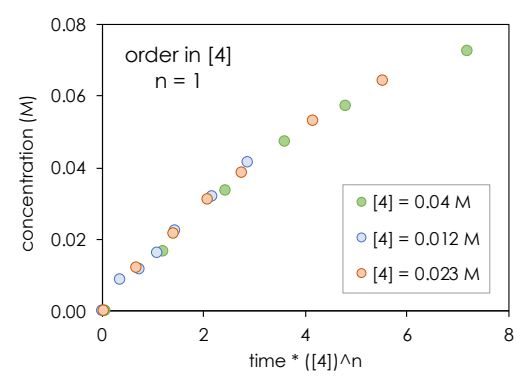


Figure 5: Variable Time Normalization Analysis¹⁴ for reactions containing varied [4] plotted as the assumed [3] against normalized-time. All reactions contain $[Pd(OAc)_2] = 0.01 \text{ M}$, [5] = 0.015 M, $[1]_0 = 0.1 \text{ M}$, $[2]_0 = 0.3 \text{ M}$, and 3.0 equiv. of AgOAc in chloroform at 80 °C. (blue circles) [4] = 0.04 M. (black circles) [4] = 0.02 M. (pink circles) [4] = 0.01 M_T

Experiments to probe the influence of additives [5] and [6] showed that the absence of 6 changed neither the enantioselectivity of the reaction nor the global rate of reaction. Reactions excluding the pyridone ligand, 5, formed product but suffered a drop in enantioselectivity of 3 and an inferior yield of product 3, (Scheme 5). Increasing concentration of 5 caused a small increase in rate up to 2 equiv compared to [Pd], while further increases in concentration of 5 diminished rate. This suggests that 5 might play a role pulling Pd off-cycle to an inactive species at high concentrations. The identity of this 5-containing off-cycle palladium species potentially could be the trimeric Pd-(5) structure (Scheme 6) previously characterized with x-ray crystallography by the Yu group. This multimeric Pd-5 species could form when Pd:5 is greater than 1:2, and this Pd complex is likely to be catalytically inactive.

Scheme 4: Pd₃(5)₅(µ²-OH) structure as determined by x-ray crystallography.⁵

Scheme 5: Reactions of Scheme 2 With and Without Pyridone 5.

entry	[5] (M)	time to 46% conversion (h)	3 %e.e.	Ratio3:7
1	0	10	64	4.75:1
2	0.015	5	85	3.60:1

In order to probe the catalyst resting state suggested by the zeroth order rate dependence on [1] and [2], we carried out reactions using **8**, a fluorine derivative of **1**, using *in-situ* ¹⁹F NMR reaction monitoring (Scheme 6). Several new ¹⁹F NMR signals (Figure 6) that were not associated with the starting material, **8**, or arylated product, **9** were observed while monitoring the Pdnorbornene (**4**)-pyridone (**5**)-catalyzed C–H arylation of **8**. An investigation of the ¹⁹F NMR literature¹⁵⁻²⁰ indicated that the signals located between -84 ppm to -96 ppm could tentatively belong to ortho-palladated aryl fluorides **10** or **13** while peaks located between -120 ppm to -124 ppm could potentially indicate the presence of para-palladated aryl fluorides **11** or **12** (.

Scheme 6: 19F-NMR Identification of Pd Species.

To determine if pyridone, 5, played a role in forming these hypothesized palladated aryl fluoride catalyst resting states, we observed the ¹⁹F NMR signals of reactions of 8 with Pd(OAc)₂ and Ag(OAc) under different conditions. The ¹⁹F NMR signals for a reaction containing 5 (Figure 6a) are significantly different for reactions that exclude 5 (Figure 6b, 6c). The ¹⁹F NMR signals in Figure 6c indicate that palladacycles 10 and 11 readily form when reacting 8 with palladium acetate in the absence of both norbornene 4 and pyridone 5. Intriguingly, the Pd-norbornene (4)-mediated C-H functionalization of 8 in the absence of pyridone, 5, still yielded product, 9, and produced ¹⁹F NMR signals that were the same as the putative signals for 10 and 11 (Figure 6b). However, these putative ¹⁹F NMR signals for **10** and 11 did not persist during the reaction of 8 with 2 in the presence of both 4 and 5, which suggests that pyridone 5 could play a role in forming the catalyst resting states 12 and 13. These insitu ¹⁹F NMR studies taken together with the zeroth order rate dependence on [1] suggest that Pd is saturated in 1 during reaction and support the involvement of the 2-pyridone ligand in the rate- and enantio-determining step.

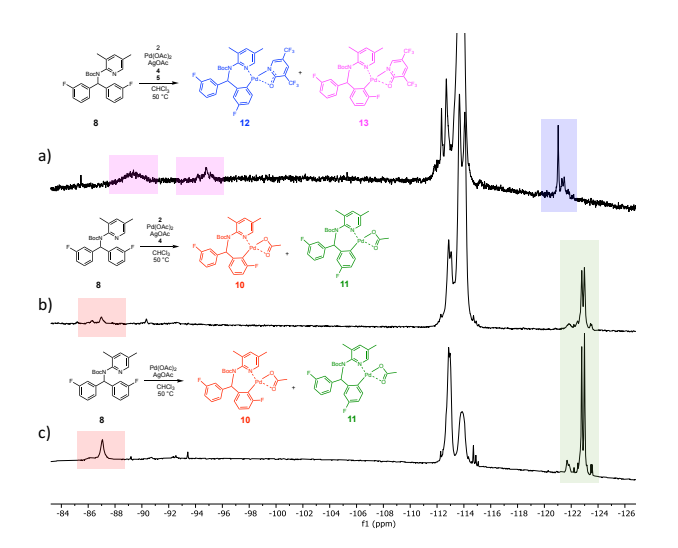


Figure 6: *In-situ* ¹⁹F NMR spectroscopy of Pd intermediates observed in reactions with substrate **8**; a) reaction between **8** with **2** in the presence of both **4** and **5**; b) reaction between **8** and **2** in the absence of pyridone **5**; c) interaction of **8** with Pd in the absence of both **4** and **5**. All reactions were conducted at 50 °C in *d*-chloroform. Hypothesized chemical structures of catalyst resting states based upon ¹⁹F NMR literature precedent. ¹⁵⁻²⁰

A reaction mechanism accounting for all these experimental observations is shown in Scheme 7. The pyridone ligand 5 brings inactive Pd-trimer on-cycle to reversibly react with 1 and form racemic intermediate 15. This arylpalladium species, 15, then undergoes rate-limiting 1,2-migratory insertion into the enantiopure norbornene, 4. The resulting insertion intermediate then goes on to react and yield product 3. The insertion of the racemic arylpalladium intermediate, 15, into the enantiopure norbornene, 4, is the first elementary step of the catalytic cycle involving a diasteroselective reaction between a racemic intermediate and a chiral reagent. The irreversibility of this diasteroselective reaction of 15 with 4 suggests that this rate-determining step is likely to also be the enantio-determining step for the reaction shown in Scheme 2. The role of the 2-pyridone ligand

within the rate-determining step is demonstrated by the previously shown ¹⁹F NMR data (Figure 8A) of an arylpalladium resting state that likely contains 5. The inferior product % *e.e.* generated under reactions that do not contain 5 also confirm the involvement of the 2-pyridone ligand in the enantio-controlling step (Scheme 6).

Scheme 7: Proposed mechanism for the reaction of Scheme 2.

CONCLUSION

In summary, our kinetics-based mechanistic investigation has revealed that the 2-pyridone ligand 5 accelerates the rate of the reaction as well as improves the product selectivity for the enantio-controlling insertion of 15 into 4. We found that stere-oselective kinetic resolution of 3 by Pd-5-6-catalyzed C(aryl)—H arylation contributes to the high % e.e. product observed at the end of the reaction. In-situ NMR spectroscopy results offer further characterization of the arylpalladium catalyst resting state for this robust Pd-catalyzed (+)-norbornene mediated meta-C(aryl)—H functionalization, supporting its role as a transient chiral mediator. The findings from this work could enable further developments in norbornene mediated meta-C(aryl)—H functionalization.

AUTHOR INFORMATION

Corresponding Author

* E-mail: blackmond@scripps.edu

Notes

The authors declare no competing financial interest. †Present address: dehill@caltech.edu

SUPPORTING INFORMATION

Details of experimental procedures, full kinetic data, NMR data.

ACKNOWLEDGMENT

This is work was supported by the National Science Foundation under the Center for Chemical Innovation Center for Selective C–H Functionalization (CHE-1700982) and by the Centre for Rapid Online Analysis of Reactions (ROAR) at Imperial College London [EPSRC, EP/R008825/1]. Dr. Jason Chen, Brittaney Sanchez, and Emily Strugell of the Scripps Automated Synthesis Center are acknowledged for valuable guidance and support on analytical methods. Prof. Mimi Hii, Dr. Benjamin Deadman, and Dr. Paola Ferrini are acknowledged for helpful discussion and support on analytical methods.

REFERENCES

- 1. Wang, P.; Farmer, M. E.; Huo, X.; Jain, P.; Shen, P.-X.; Ishoey, M.; Bradner, J. E.; Wisniewski, S. R.; Eastgate, M. D.; Yu, J.-Q., Ligand-Promoted *meta*-C–H Arylation of Anilines, Phenols, and Heterocycles. *J. Am. Chem. Soc.* **2016**, *138*, 9269-9276.
- 2. Wang, P.; Li, G.-C.; Jain, P.; Farmer, M. E.; He, J.; Shen, P.-X.; Yu, J.-Q., Ligand-Promoted *meta-C*–H Amination and Alkynylation. *J. Am. Chem. Soc.* **2016**, *138*, 14092-14099.
- 3. Shi, H.; Wang, P.; Suzuki, S.; Farmer, M. E.; Yu, J.-Q., Ligand Promoted *meta*-C–H Chlorination of Anilines and Phenols. *J. Am. Chem. Soc.* **2016**, *138*, 14876-14879.
- 4. Li, G.-C.; Wang, P.; Farmer, M. E.; Yu, J.-Q., Ligand-Enabled Auxiliary-Free *meta*-C-H Arylation of Phenylacetic Acids. *Angew. Chem. Int. Ed.* **2017**, *56*, 6874-6877.
- 5. Wang, P.; Verma, P.; Xia, G.; Shi, J.; Qiao, J. X.; Tao, S.; Cheng, P. T. W.; Poss, M. A.; Farmer, M. E.; Yeung, K.-S.; Yu, J.-Q., Ligand-Accelerated Non-Directed C–H Functionalization of Arenes. *Nature.* **2017**, *551*, 489.
- 6. Zhu, R.-Y.; Li, Z.-Q.; Park, H. S.; Senanayake, C. H.; Yu, J.-Q., Ligand-Enabled γ -C(sp³)–H Activation of Ketones. *J. Am. Chem. Soc.* **2018**, *140*, 3564-3568.
- 7. Shi, H.; Herron, A. N.; Shao, Y.; Shao, Q.; Yu, J.-Q., Enantioselective Remote *meta*-C–H Arylation and Alkylation via a Chiral Transient Mediator. *Nature*. **2018**, *558*, 581-585.
- 8. Farmer, M. E.; Wang, P.; Shi, H.; Yu, J.-Q., Palladium-Catalyzed *meta*-C–H Functionalization of Masked Aromatic Aldehydes. *ACS Catal.* **2018**, *8*, 7362-7367.

- 9. Liu, L.-Y.; Yeung, K.-S.; Yu, J.-Q., Ligand-Promoted Non-Directed C-H Cyanation of Arenes. *Chem. Eur. J.* **2019**, *25*, 2199-2202.
- 10. Wang, J.; Dong, G., Palladium/Norbornene Cooperative Catalysis. *Chem. Rev.* **2019**, *119*, 7478-7528.
- 11. Catellani, M.; Motti, E.; Della Ca', N., Catalytic Sequential Reactions Involving Palladacycle-Directed Aryl Coupling Steps. *Acc. Chem. Res.* **2008**, *41*, 1512-1522.
- 12. Blackmond, D. G., Reaction Progress Kinetic Analysis: A Powerful Methodology for Mechanistic Studies of Complex Catalytic Reactions. *Angew. Chem. Int. Ed.* **2005**, *44*, 4302-4320.
- 13. Mathew, J. S.; Klussmann, M.; Iwamura, H.; Valera, F.; Futran, A.; Emanuelsson, E. A. C.; Blackmond, D. G., Investigations of Pd-Catalyzed ArX Coupling Reactions Informed by Reaction Progress Kinetic Analysis. *J. Org. Chem.* **2006**, *71*, 4711-4722.
- 14. Burés, J., A Simple Graphical Method to Determine the Order in Catalyst. *Angew. Chem. Int. Ed.* **2016,** *55*, 2028-2031.
- 15. Ball, N. D.; Kampf, J. W.; Sanford, M. S., Aryl–CF3 Bond-Forming Reductive Elimination from Palladium(IV). *J. Am. Chem. Soc.* **2010**, *132*, 2878-2879.
- 16. Scharf, A.; Goldberg, I.; Vigalok, A.; Vedernikov, A. N., Aryl-F Bond Cleavage vs. C–E Reductive Elimination: Competitive Pathways of Metal–Ligand-Cooperation-Based E–H Bond Activation (E = N, S). *European Journal of Inorganic Chemistry*. **2015**, *2015*, 4761-4768.
- 17. Neukom, J. D.; Perch, N. S.; Wolfe, J. P., Intramolecular Insertion of Alkenes into Pd–N Bonds. Effects of Substrate and Ligand Structure on the Reactivity of (P–P)Pd(Ar)[N(Ar₁)(CH₂)₃CR=CHR'] Complexes. *Organometallics.* **2011**, *30*, 1269-1277.
- 18. Carrow, B. P.; Hartwig, J. F., Ligandless, Anionic, Arylpalladium Halide Intermediates in the Heck Reaction. *J. Am. Chem. Soc.* **2010**, *132*, 79-81.
- 19. Thomas, A. A.; Wang, H.; Zahrt, A. F.; Denmark, S. E., Structural, Kinetic, and Computational Characterization of the Elusive Arylpalladium(II)boronate Complexes in the Suzuki–Miyaura Reaction. *J. Am. Chem. Soc.* **2017**, *139*, 3805-3821.
- 20. Sgro, M. J.; Stephan, D. W., Ni(II), Pd(II) and Pt(II) complexes of PNP and PSP tridentate amino–phosphine ligands. *Dalton Transactions.* **2012**, *41*, 6791-6802.